Development of magnetic order in the TbNi(Al,In) series and magnetocrystalline anisotropy in TbTX compounds

M. Klicpera,[1,*] P. Javorský,[1] and I. Puente Orench[2,3]

[1]*Charles University, Faculty of Mathematics and Physics, Department of Condensed Matter Physics,
Ke Karlovu 5, CZ-121 16 Prague 2, Czech Republic*
[2]*Institut Laue Langevin, 6 rue Jules Horowitz, FR-38042 Grenoble Cedex 9, France*
[3]*Instituto de Ciencia de Materiales de Aragón ICMA-CSIC, Pedro Cerbuna 12, ES-50009 Zaragoza, Spain*

We report on the magnetic structures in the TbNiAl$_{1-x}$In$_x$ compounds as determined by powder neutron diffraction. These compounds belong to a large family of ternary rare-earth intermetallics crystallizing in the ZrNiAl-type hexagonal structure. All studied compounds order magnetically with magnetic structures characterized by $\mathbf{k}_1 = (0,0,0)$ and $\mathbf{k}_2 = (\frac{1}{2},0,\frac{1}{2})$ propagation vectors and magnetic moments aligned along or perpendicular to the hexagonal c axis. The magnetocrystalline anisotropy changes from uniaxial in the In-poor compounds ($x \leqslant 0.4$) to planar in the In-rich compounds ($x \geqslant 0.5$). The change of magnetocrystalline anisotropy type is a consequence of the development of structural parameters in the studied series. The Tb moments are oriented along the c axis when the nearest Tb-Tb distances between the planes are large compared to those within the planes, whereas Tb moments lie within the basal planes in the opposite case. This picture relating the structural parameters and anisotropy type can be generalized to the whole group of Tb-based compounds with the ZrNiAl type of structure.

I. INTRODUCTION

The rare-earth intermetallic compounds often order magnetically at low temperatures showing various types of magnetic structures. In compounds where only the rare-earth ions bear the magnetic moments, the magnetic order appears mainly as a result of indirect exchange interactions between the rare-earth moments and the influence of crystal field. The magnetic and other physical properties can be relatively easily modified by substitutions of individual elements in these compounds. The substitutions lead to (i) change of the number of electrons in the system and (ii) change of the crystallographic parameters, assuming that the structure type itself remains unchanged. In this way, not only can the physical properties be changed to desired ones, but the investigation of the effect of substitutions can also lead to a better understanding of microscopic mechanisms that are responsible for the observed behavior. The existence of a broad family of compounds with the same crystallographic structure is a prerequisite for such systematic investigation of substitutional effects.

The RTX compounds (R = rare earth, T = late transition metal, X = p-metal) crystallizing in the hexagonal ZrNiAl-type of structure (see Fig. 1) form a large group of materials suitable for the above-mentioned systematic investigations. From the structural point of view, it is interesting to note an abrupt change of the lattice parameters a and c observed in the temperature or composition dependence with the common feature that the values of the c/a ratio around $0.565 - 0.575$ are generally not realized.[1] It has been shown[1] that this structural transition has only a little effect on the magnetic properties. The magnetic behavior of these RTX compounds is rather complex. Most of these compounds order magnetically at low temperatures with magnetic structures often characterized by frustration due to a triangular arrangement of the rare-earth ions in the crystal structure.[2] Several substitutional series were

studied to follow the development of magnetic properties. The change of conduction-electron number, like in the R(Ni,Cu)Al series, has a dramatic impact on the magnetic behavior,[3–5] including the loss of long-range magnetic order in a certain concentration range of R(Ni,Cu)Al compounds and also the appearance of the spin-glass state.[5] On the other hand, the isoelectronic substitution in Tb(Ni,Pd)Al series leads only to changes of the magnetic properties. Here we have to mention that both structural parameters, a and c, change considerably in the Tb(Ni,Pd)Al series, but the c/a ratio remains nearly unchanged. Simultaneous change of the c/a ratio and the electron number was investigated in the Er(Au,Ni)In compounds revealing also rather complex development, including a change of the magnetocrystalline anisotropy type.[6]

The subject of this paper is the development of magnetic properties in the TbNi(Al,In) series. The type of anisotropy is expected to change between easy-axis type (TbNiAl)[7] and easy-plane type (TbNiIn).[8] Because the Al-In substitution is isoelectronic, we expect that changes of the magnetic properties are primarily driven by the structural changes which are here much more significant than in previously studied Tb(Ni,Pd)Al or Er(Au,Ni)In (see below the results of crystal structure).

TbNiAl has been a subject of intensive studies by means of different experimental techniques.[7,9–13] This compound orders antiferromagnetically below $T_N \cong 45$ K and undergoes further magnetic phase transition at $T_1 = 23$ K. Neutron diffraction studies on polycrystalline samples[9] and on single crystal[7] reveal that the antiferromagnetic order in TbNiAl is characterized by a propagation vector $(\frac{1}{2},0,\frac{1}{2})$ with Tb magnetic moments oriented along the c axis in both magnetic phases. One-third of the moments is strongly reduced to almost zero between T_N and T_1 due to a geometrical frustration. The frustrated moments start to propagate along different equivalent directions, for example, with propagation vector $(0,\frac{1}{2},\frac{1}{2})$ below T_1. The strong frustration is removed below

T_1 and finally all Tb moments reach the same value at 2 K.[7] The large magnetocrystalline anisotropy with an anisotropy field above 35 T was demonstrated by magnetization measurements on a single crystal.[7] The metamagnetic transition to a ferromagnetic state occurs when applying an external magnetic field of $\simeq 0.4$ T along the c axis at 2 K, whereas the magnetic structure is almost insensitive to magnetic fields applied perpendicular to the c axis.[7] The strong magnetocrystalline anisotropy reflects also in a highly anisotropic magnetocaloric properties.[14]

The magnetic properties of TbNiIn have been studied less intensively. Magnetization and ac-susceptibility measurements revealed magnetic order below $T_{\rm ord} \cong 70$ K.[15,16] Additional magnetic phase transitions at $T' = 59$ K and $T_1 = 29$ K were furthermore indicated by anomalies observed in ac-susceptibility data.[15] Our recent magnetic bulk measurements[17] showed similar features with slightly different transition temperatures: $T_{\rm ord} = 72$ K, $T' = 54$ K, and $T_1 = 20$ K. In the paramagnetic region, the magnetization follows the Curie-Weiss law with positive $\theta_{\rm P} = 55$ K and the effective moment close to the Tb^{3+} free-ion value. Powder neutron diffraction experiments revealed two magnetic phases with transition temperatures of $T_{\rm ord} = 68$ K and $T_1 = 32$ K (Ref. [8]). The magnetic structure below $T_{\rm ord}$ is described by (0,0,0) propagation vector and the Tb moments form a noncollinear structure with angle of $120°$ between nearest neighboring moments. Additional weaker component with $(\frac{1}{2},0,\frac{1}{2})$ propagation develops below T_1, but no details were provided for the orientation of these components.[8]

Our previous investigations of the TbNiAl$_{1-x}$In$_x$ series show monotonous change of the lattice parameters with a strong change of the c/a ratio. The bulk magnetization measurements[17] show relatively weak concentration dependence of the ordering temperatures and reveal the existence of two ($x \leqslant 0.7$) or three ($x \geqslant 0.8$) magnetic phases. The low-temperature x-ray diffraction measured on powder samples in a magnetic field of 0.3 T (Ref. [18]) proves the monotonous change of lattice parameters also in the magnetically ordered state at 20 K. Moreover, the appearance or absence of strong uniaxial texture of the powder grains observed in this low-temperature experiment indicated the change of the magnetocrystalline anisotropy type from uniaxial to planar for concentrations with x around 0.3 (Ref. [18]). In the present work, we describe the magnetic structures as determined from powder neutron diffraction. We present also a general picture of the type of magnetocrystalline anisotropy in the hexagonal TbTX compounds.

II. EXPERIMENTAL

Polycrystalline TbNiAl$_{1-x}$In$_x$ samples, where x ranges from 0.0 to 1.0 with a step of 0.1, were prepared by arc melting pure elements (3N for Tb, 4N5 for Ni, 5N for Al, and 6N for In) in a mono-arc furnace under the protection of an argon atmosphere. We add $\sim 5\%$ of In to account for higher evaporation of In (approximately two or three orders of magnitude compared to other used elements). The samples were turned and remelted four times to obtain better homogeneity. All the samples were additionally sealed in
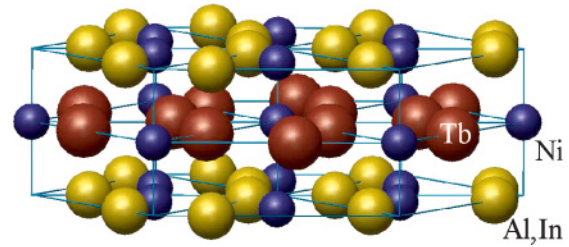

FIG. 1. (Color online) The hexagonal ZrNiAl type of structure (space group $P\bar{6}2m$) adopted by the TbNi(Al,In) compounds.

silicon glass under pressure of 10^{-4} Pa and then annealed for 10 days at 650 °C.

The x-ray diffraction patterns at room temperature were measured to verify the crystal structure and to refine the structural parameters. The analysis of the diffraction data showed that the main phase is a ZrNiAl-type structure (see Fig. [1]). The few weak additional peaks indicate the presence of a small amount of impurity phase(s). The chemical composition was subsequently investigated by a scanning electron microscope equipped with a backscattered electron (BSE) detector and with an energy dispersive x-ray (EDX) analyzer. The analysis showed that the samples are composed predominantly by the main phase with a small admixture ($<5\%$) of the secondary phase, in agreement with the x-ray analysis. The minority phase has approximately the following composition: Tb:Ni:Al(In) = 1:2:2 or 2:4:3. We did not find in the literature any compound with similar composition.

The powder neutron-diffraction experiment was performed at the Institute Laue-Langevin, using the D1B instrument. The diffracted neutrons with a wavelength of 2.53 Å were detected over an angular range of 80° using a multidetector with a step of 0.2° between each of the 400 ^{3}He detection cells. The powder samples (with the weight of $3-4$ g) were placed in cylindrical vanadium containers of 5.7 mm diameter and 50 mm height. The diffraction patterns were taken for 9 concentrations from the TbNiAl$_{1-x}$In$_x$ series (not measured for $x = 0.0$ and 0.7). Patterns with high statistics were measured at temperatures corresponding to every magnetic phase as expected from the magnetization and specific-heat data,[17] that is, at 2 K, 30 K, or 35 K, depending on its In concentration, and also at the paramagnetic region. Additionally, except for samples with $x = 0.1$ and 0.6, diffraction patterns with slightly lower statistics were recorded while heating from 2 K up to the paramagnetic state every 2 K or 3 K in order to follow the development of the changes with temperature in more detail. The refinement of the powder neutron diffraction patterns was done using the FULLPROF program employing the Rietveld analysis[19] with the absorption coefficients taken from Ref. [20]. Possible preferential orientation of the crystallites was also included during the refinement. We have used the MARCH function[21] that is implemented in the FULLPROF program. Our refinement revealed weak preferential orientation that takes the plate-shape form for all concentrations, except for TbNiAl$_{0.5}$In$_{0.5}$ and TbNiIn samples, which do not show any preferential orientation. Representation analysis to determine possible magnetic structures was performed using the computer program SARAh.[22]

III. RESULTS

A. Crystal structure

The diffraction patterns recorded at the paramagnetic state (between 60 K and 80 K, depending on In concentration) confirmed the hexagonal ZrNiAl type of structure. This crystal structure, shown in Fig. 1, consists of two types of layers at $z = 0$ and $\frac{1}{2}$, with the following atomic positions:

3Tb in 3(g): $(x_{Tb}, 0, \frac{1}{2})$, $(0, x_{Tb}, \frac{1}{2})$, $(-x_{Tb}, -x_{Tb}, \frac{1}{2})$,

3Al(In) in 3(f): $(x_{Al}, 0, 0)$, $(0, x_{Al}, 0)$, $(-x_{Al}, -x_{Al}, 0)$,

2Ni in 2(c): $(\frac{1}{3}, \frac{2}{3}, 0)$, $(\frac{2}{3}, \frac{1}{3}, 0)$,

1Ni in 1(b): $(0, 0, \frac{1}{2})$.

The diffraction patterns of $TbNiAl_{0.9}In_{0.1}$ and $TbNiAl_{0.2}In_{0.8}$ are shown in Figs. 2 and 3 as an example. Beside the nuclear reflections of the main hexagonal phase, we observe a few spurious weak peaks (marked by "*" in Figs. 2 and 3) which probably correspond to the presence of the minority phase in the sample as indicated also by EDX analysis. The positions of the impurity phase peaks in neutron diffraction patterns correspond to those observed also in the x-ray diffraction patterns. The number and low intensity of these peaks did not allow us to determine corresponding crystal structure of this minority phase(s). The peak around $2\theta = 72°$ is due to the vanadium sample container (labeled "V").
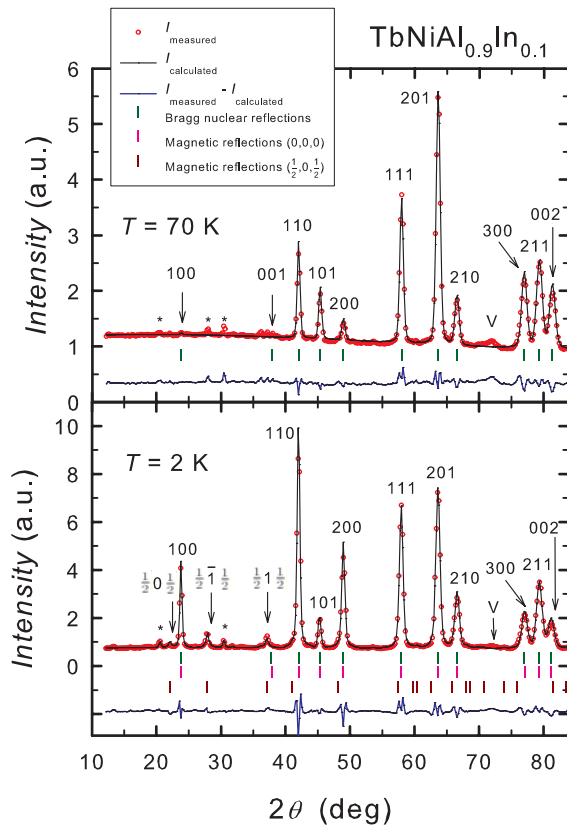

FIG. 2. (Color online) Diffraction patterns of $TbNiAl_{0.9}In_{0.1}$ compound at 2 K and 70 K. The vertical bars below the diffraction patters mark the reflections described by propagation vectors $\mathbf{k}_1 = (0,0,0)$ and $\mathbf{k}_2 = (\frac{1}{2},0,\frac{1}{2})$. The weak peaks marked by "*" symbols are due to an impurity phase.

FIG. 3. (Color online) Diffraction patterns of $TbNiAl_{0.2}In_{0.8}$ compound at 2 K and 70 K. The vertical bars below the diffraction patters mark the reflections described by propagation vectors $\mathbf{k}_1 = (0,0,0)$ and $\mathbf{k}_2 = (\frac{1}{2},0,\frac{1}{2})$. The weak peaks marked by "*" symbols are due to an impurity phase.
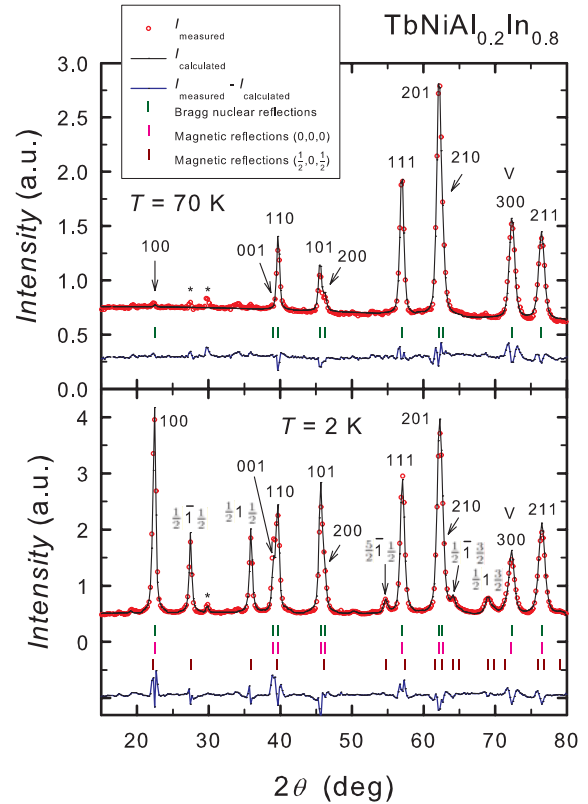
The refinement of our data led to structural parameters summarized in Table I. The lattice parameter a increases linearly with increasing indium content, whereas the parameter c decreases linearly between concentrations $x = 0.0$ and 0.8 and remains almost unchanged for higher In concentrations. This development of lattice parameters obtained by neutron diffraction at temperatures slightly above the magnetic phase transition is in agreement with results obtained using the x-ray diffraction at room temperature and at 20 K (Ref. 18). The atomic position parameters of Tb and Al(In) atoms remain almost concentration independent except for a slight increase of $x_{Al,In}$ in concentrations with $x \geqslant 0.5$.

The Tb-Tb interatomic distances within the basal plane can be calculated as

$$d_{BP} = a\sqrt{1 - 3x - 3x^2}. \tag{1}$$

As can be seen from Table I, the Tb-Tb nearest-neighbor distance is within the basal plane for $x \leqslant 0.6$ and along the c axis for $x > 0.6$. It is a consequence of the strong development of the c/a ratio. These structural changes give rise to a change of the magnetocrystalline anisotropy type, as we show below.

B. Magnetic structures

Below the temperature of magnetic ordering T_{ord}, we observe the development of additional intensities (see Figs. 2 and 3). The most intense is the increase of intensity on positions of

TABLE I. Lattice parameters of TbNiAl$_{1-x}$In$_x$ compounds in the paramagnetic state (i.e., 60 K – 80 K) determined from powder neutron diffraction. $V_{\text{f.u.}}$ is the volume; d_{BP} means the Tb-Tb distance in the basal plane; x_{Tb} and $x_{\text{Al(In)}}$ are fraction coordinates of Tb and Al(In) atoms in the fundamental unit; R_{Bragg} is the agreement factor for the nuclear fit.

x	T (K)	a (pm)	c (pm)	d_{BP}	c/a	$V_{\text{f.u.}}$ (10^6 pm^3)	x_{Tb}	$x_{\text{Al(In)}}$	R_{Bragg} (%)
0.1	70	703.0(2)	387.6(1)	364.7(2)	0.5513(2)	51.97(4)	0.582(1)	0.238(2)	4.1
0.2	60	708.2(3)	385.6(1)	367.4(3)	0.5445(3)	52.48(6)	0.580(1)	0.239(4)	5.9
0.3	60	714.1(3)	383.7(1)	370.5(3)	0.5373(2)	53.11(6)	0.579(1)	0.239(3)	6.0
0.4	70	720.0(3)	382.1(1)	373.6(3)	0.5306(2)	53.76(6)	0.584(1)	0.240(3)	4.7
0.5	70	724.5(3)	380.9(2)	375.9(3)	0.5258(3)	54.26(9)	0.579(2)	0.245(4)	6.9
0.6	70	730.7(3)	379.5(2)	379.1(3)	0.5194(3)	54.99(8)	0.583(2)	0.248(4)	5.5
0.8	70	740.3(3)	377.1(2)	384.1(3)	0.5094(2)	56.09(7)	0.588(1)	0.259(3)	6.7
0.9	80	744.3(3)	377.0(2)	386.2(3)	0.5064(3)	56.68(9)	0.585(2)	0.259(4)	6.4
1.0	80	744.9(2)	378.0(2)	386.8(2)	0.5052(1)	56.93(6)	0.592(1)	0.260(3)	4.8

nuclear reflections when decreasing temperature. These magnetic reflections are described by the propagation vector $\mathbf{k}_1 = (0,0,0)$. Further, purely magnetic peaks observed at 2 K can be described by the propagation vector $\mathbf{k}_2 = (\frac{1}{2},0,\frac{1}{2})$, which occurs also in pure TbNiAl. Magnetic reflections described by these two propagation vectors are observed for all concentrations. Although the propagation vectors are the same, the directions of Tb magnetic moments differ. This is well demonstrated on Fig. 4. There is no magnetic intensity on the (001) reflection for TbNiAl$_{0.6}$In$_{0.4}$, whereas (001) is a very strong magnetic peak for the TbNiAl$_{0.5}$In$_{0.5}$ compound. Such an observation immediately suggests an idea that Tb moments (those described by $\mathbf{k}_1$) are parallel to the c axis in TbNiAl$_{0.6}$In$_{0.4}$ and perpendicular to the c axis in the TbNiAl$_{0.5}$In$_{0.5}$ compound. According to the moment direction, we distinguish thus two concentration ranges: $x \leqslant 0.4$ and $x \geqslant 0.5$.

To avoid any ambiguity with respect to our previously published results,[17] we specify the notation of magnetic phase transition temperatures. In Table II and in the following text we take the values of transition temperatures as determined from bulk measurements[17] but change the notation to reflect the microscopic nature of these transitions. We denote as T_1 the temperature which is related to increase or changes of the antiferromagnetic component described by $\mathbf{k}_2 = (\frac{1}{2},0,\frac{1}{2})$. The T' then labels possible transition observed for $x \geqslant 0.8$

between T_{ord} and T_1, which is discussed below. The remaining transition temperature observed as rather weak anomalies in bulk measurements[17] for several concentrations below T_1 does not correspond to any changes of diffraction patterns and most probably is due to the impurity phase.

Let us first describe magnetic structures in In-poor compounds with $x \leqslant 0.4$. The diffraction patterns of these compounds are all rather similar, including the temperature development (see Fig. 5). First, the magnetic intensities with $\mathbf{k}_1 = (0,0,0)$ develop below the ordering temperature, increase strongly down to T_1, and stay almost constant below T_1, as can be seen on Fig. 5. The symmetry-allowed magnetic structures for this propagation vector are listed in Table III. We have furthermore considered that in cases where the irreducible representation contains more than one basis vector, the combination of two or more of these basis vectors represents allowed magnetic moment arrangements as well. The refinement of diffraction patterns in the whole temperature range down to 2 K points to collinear ferromagnetic structure with magnetic moments oriented along the c axis [Γ_3 in Table III and Fig. 6(A)]. The values of corresponding magnetic moments at selected temperatures are summarized in Table IV; the calculated pattern is shown in Fig. 2 for TbNiAl$_{0.9}$In$_{0.1}$. Slight improvement of the fit (magnetic phase agreement factor for fit, R_{M}, is improved by ~ 0.2 at 2 K) is achieved when allowing small deviation ($4° – 7°$, depending on concentration) of the moment direction from the c axis. This deviation is in
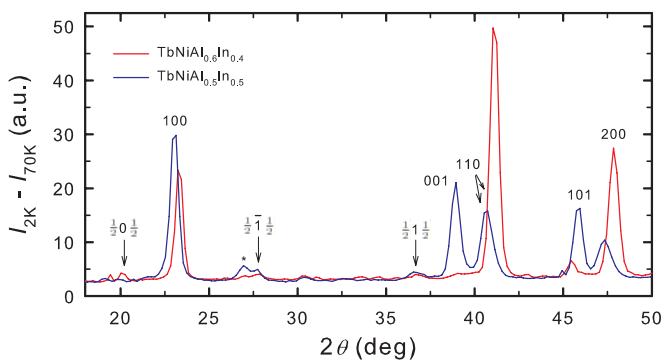

FIG. 4. (Color online) Differential diffraction patterns of TbNiAl$_{0.6}$In$_{0.4}$ and TbNiAl$_{0.5}$In$_{0.5}$ obtained by the subtracting the paramagnetic data from data obtained at 2 K. The strongest magnetic peaks are indexed, the peak marked by "*" is due to an impurity phase.

TABLE II. Temperatures of magnetic phase transitions of TbNiAl$_{1-x}$In$_x$ compounds obtained from bulk measurement[17] (see text for more details).

x	T_{ord} (K)	T' (K)	T_1 (K)
0.1	48		25
0.2	48		22
0.3	45		15
0.4	42		12
0.5	42		12
0.6	45		14
0.8	56	52	20
0.9	60	49	21
1.0	72	54	20

conflict with the symmetry-allowed structures. Because of that and because the improvement of the fit is very small, we are inclined to conclude that magnetic structure with moments parallel to the c axis is realized for these In-poor compounds.

The magnetic intensities described by $\mathbf{k}_2 = (\frac{1}{2}, 0, \frac{1}{2})$ are rather weak in all of these In-poor compounds. They emerge as very small peaks far above T_1 as previously determined from bulk measurements (see Fig. 5).[17] At around T_1, intensity ratios of several observable peaks change and the peaks become stronger. However, the intensities are too small to determine unambiguously the corresponding magnetic structures and the nature of the transition at T_1. We can only conclude that the corresponding moments lie within the basal plane. The best agreement with the experimental data is obtained for the magnetic arrangement drawn in Fig. 6(a), which is also in agreement with the representation analysis reported for this propagation vector.[7] The corresponding calculated curve is represented in Fig. 2 for TbNiAl$_{0.9}$In$_{0.1}$. The fit with moments along the c axis is substantially worse. Furthermore, the fit leads to the moment size of about 2 $\mu_{\rm B}$, independently on the direction. Considering both components propagating with $\mathbf{k}_1$ and $\mathbf{k}_2$ to lie parallel along the c axis, the total Tb moment would exceed considerably the full Tb^{3+} free ion value of 9 $\mu_{\rm B}$. The magnetic order at 2 K for compounds with $x \leqslant 0.4$ can be thus described as a canted magnetic structure with
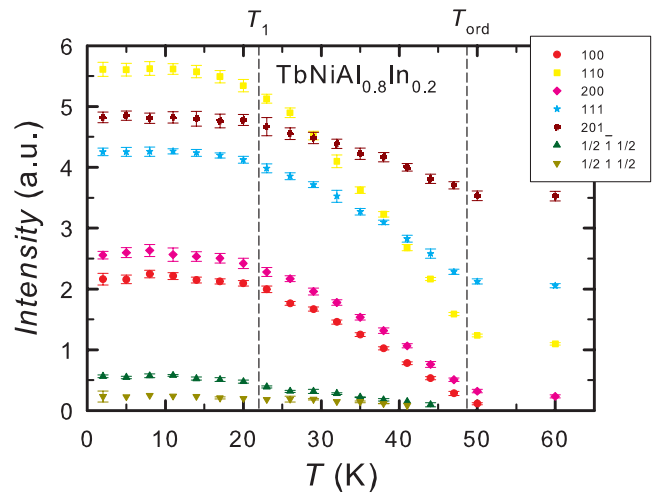

FIG. 5. (Color online) The temperature dependence of the intensity of the strongest reflections in TbNiAl$_{0.8}$In$_{0.2}$ compound. Dashed lines mark the temperatures of magnetic phase transitions as indicated by bulk measurements.[17]

dominant ferromagnetic component along the c axis and a much weaker antiferromagnetic basal-plane component with $\mathbf{k}_2 = (\frac{1}{2}, 0, \frac{1}{2})$. Such magnetic structures occur in several other RTX compounds.[2,23,24]
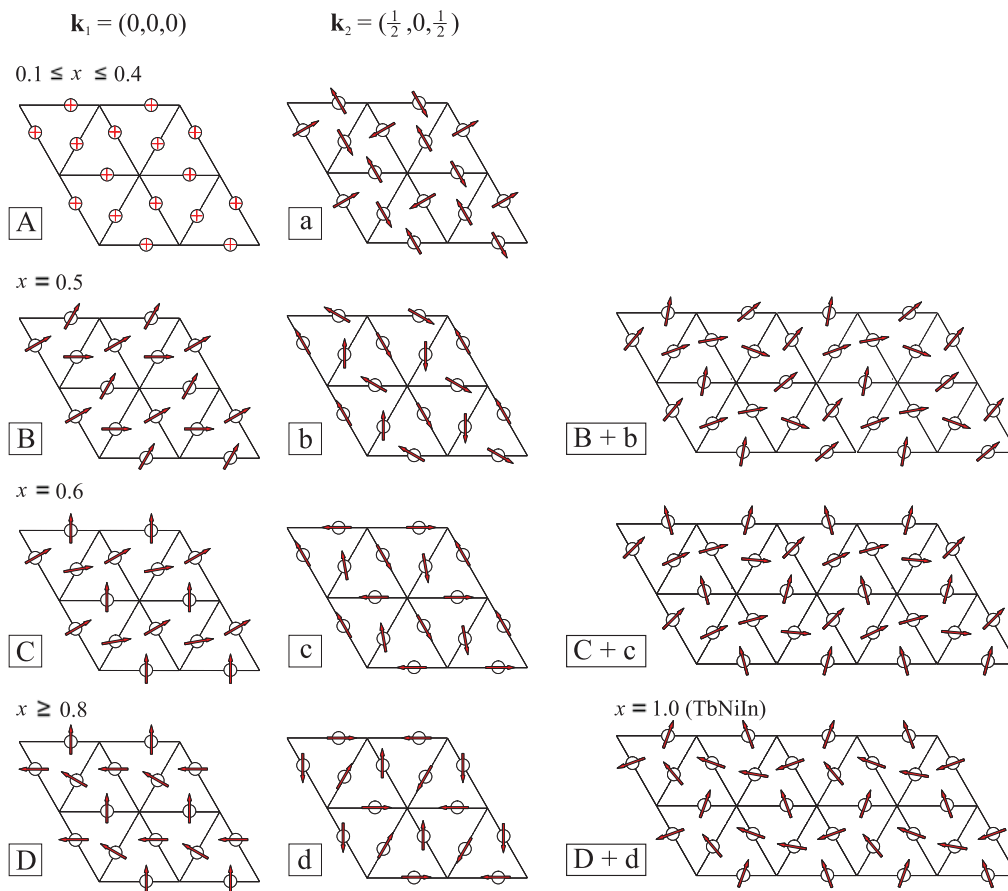

FIG. 6. (Color online) Magnetic structures occurring in TbNiAl$_{1-x}$In$_x$ series at 2 K. The arrangement of the moments drawn in the first column belongs to propagation vector $\mathbf{k}_1 = (0,0,0)$; in the second column it belongs to $\mathbf{k}_2 = (\frac{1}{2}, 0, \frac{1}{2})$. The third column contains the total magnetic structures obtained by adding together the two components of magnetic moment, considering the actual size of both components at 2 K. The A–D and a–d labels correspond to the notation in Table IV. The "D + d" structure reflects the values of TbNiIn only.

TABLE III. Basis vectors of the irreducible representations for a $\mathbf{k}_1 = (0,0,0)$ propagation vector as obtained by the SARAh program.[22]

Irreducible representation	Tb atomic position		
	$(x_{\mathrm{Tb}}, 0, \frac{1}{2})$	$(0, x_{\mathrm{Tb}}, \frac{1}{2})$	$(-x_{\mathrm{Tb}}, -x_{\mathrm{Tb}}, \frac{1}{2})$
Γ_2	$(1, 0, 0)$	$(0, 1, 0)$	$(-1, -1, 0)$
Γ_3	$(0, 0, 1)$	$(0, 0, 1)$	$(0, 0, 1)$
Γ_4	$(1, 2, 0)$	$(-2, -1, 0)$	$(1, -1, 0)$
Γ_5	$(0, 0, 3)$	$(0, 0, 0)$	$(0, 0, -3)$
Γ_5	$(0, 0, \sqrt{3})$	$(0, 0, -2\sqrt{3})$	$(0, 0, \sqrt{3})$
Γ_6	$(1, 0, 0)$	$(0, -2, 0)$	$(-1, -1, 0)$
Γ_6	$(1, 3, 0)$	$(0, 1, 0)$	$(-1, 2, 0)$
Γ_6	$(-\sqrt{3}, 0, 0)$	$(0, 0, 0)$	$(-\sqrt{3}, -\sqrt{3}, 0)$
Γ_6	$(\sqrt{3}, \sqrt{3}, 0)$	$(2\sqrt{3}, \sqrt{3}, 0)$	$(\sqrt{3}, 0, 0)$

The diffraction patterns in compounds with $x \geqslant 0.5$ change significantly compared with low-In-concentration diffraction records (see Fig. 4). Let us first describe the magnetic structures related to the $\mathbf{k}_1 = (0,0,0)$ propagation which is again dominant. We note that the $(0,0,0)$ propagation does not imply unambiguously a ferromagnetic order because there are three Tb atoms in the unit cell. The refinement of the observed patterns leads to the magnetic structures summarized in Table IV and Fig. 6. The corresponding magnetic moments lie within the basal plane for all compounds with $x \geqslant 0.5$. The magnetic structure in TbNiAl$_{0.5}$In$_{0.5}$ is well in agreement with the representation analysis [compare Fig. 6(B) and Γ_6 representation with the basis vector in the last row of Table III]. The magnetic structures determined for the other compositions ($x = 0.6, 0.8$, 0.9, and 1.0) differ somewhat from the representation analysis results. Nevertheless, we are inclined to the refined structures because the agreement with the observed data improves significantly compared to any symmetry-allowed structure: R_{M} is improved at least by $\sim$10% at 2 K. Concerning the pure TbNiIn, the difference with respect to the previously published result described as noncollinear structure with the angle of $120°$ between nearest-neighboring Tb moments[8] could be due to sample imperfections (possibly on both sides). The sample dependence of some details of magnetic structures was already observed in this family of RTX compounds.[23]

The intensity of reflections belonging to $\mathbf{k}_2 = (\frac{1}{2}, 0, \frac{1}{2})$ remained also very small, except for TbNiAl$_{0.2}$In$_{0.8}$ and TbNiAl$_{0.1}$In$_{0.9}$. These intensities develop around T_1, as can be seen from Figs. 7 and 8. The refinement of corresponding magnetic structures is rather complicated not only because of small intensities, but also due to an overlap of several of these peaks with stronger peaks belonging to $(0,0,0)$ propagation. For example, the $(\frac{1}{2}0\frac{1}{2})$ reflection appears on almost the same angle as the stronger (100) reflection (see Fig. 3). The maximum value of the full Tb^{3+} moment is another criterion which should be taken into account when refining the magnetic structure. The magnetic moment on a single Tb atom should not exceed 9 μ_{B}. Considering this restraint, the best agreement of the fit with measured data was obtained for the magnetic structures summarized in Table IV and Fig. 6. The components described by $\mathbf{k}_2$ are always perpendicular to those described by $\mathbf{k}_1$, which is a quite natural conclusion. The total Tb moments

TABLE IV. Parameters of magnetic structures of TbNiAl$_{1-x}$In$_x$ compounds determined from powder neutron diffraction at selected temperatures in individual magnetic phases as indicated by bulk measurements.[17] μ is the magnetic moment of the phase belonging to propagation vector $\mathbf{k}$; R_{M} is agreement factor for the fit of magnetic phase. Letters A–D and a–d represent the magnetic structures drawn in Fig. 6. The symbol "*" means that magnetic peaks are too weak to determine the magnetic structure unambiguously.

x	T (K)	$\mathbf{k}$	Structure type	μ (μ_{B})	R_{M} (%)
0.1	2	$(0,0,0)$	$\vec{\mu} \parallel \vec{c}$, A	8.4(1)	4.7
		$(\frac{1}{2},0,\frac{1}{2})$	$\vec{\mu} \perp \vec{c}$, a*	2.0(2)	27.2
	30	$(0,0,0)$	$\vec{\mu} \parallel \vec{c}$, A	7.1(1)	4.7
		$(\frac{1}{2},0,\frac{1}{2})$	$\vec{\mu} \perp \vec{c}$, a*	1.5(3)	40.4
0.2	2	$(0,0,0)$	$\vec{\mu} \parallel \vec{c}$, A	7.9(1)	4.6
		$(\frac{1}{2},0,\frac{1}{2})$	$\vec{\mu} \perp \vec{c}$, a*	2.2(2)	35.5
	35	$(0,0,0)$	$\vec{\mu} \parallel \vec{c}$, A	5.8(1)	5.0
		$(\frac{1}{2},0,\frac{1}{2})$	$\vec{\mu} \perp \vec{c}$, a*	1.0(3)	73.0
0.3	2	$(0,0,0)$	$\vec{\mu} \parallel \vec{c}$, A	8.2(1)	5.6
		$(\frac{1}{2},0,\frac{1}{2})$	$\vec{\mu} \perp \vec{c}$, a*	2.2(2)	42.9
	30	$(0,0,0)$	$\vec{\mu} \parallel \vec{c}$, A	6.7(1)	4.2
		$(\frac{1}{2},0,\frac{1}{2})$	$\vec{\mu} \perp \vec{c}$, a*	1.5(3)	51.7
0.4	2	$(0,0,0)$	$\vec{\mu} \parallel \vec{c}$, A	8.3(1)	5.7
		$(\frac{1}{2},0,\frac{1}{2})$	$\vec{\mu} \perp \vec{c}$, a*	1.8(2)	61.0
	30	$(0,0,0)$	$\vec{\mu} \parallel \vec{c}$, A	5.9(1)	6.8
		$(\frac{1}{2},0,\frac{1}{2})$	$\vec{\mu} \perp \vec{c}$, a*	0.8(2)	81.0
0.5	2	$(0,0,0)$	$\vec{\mu} \perp \vec{c}$, B	8.2(1)	7.6
		$(\frac{1}{2},0,\frac{1}{2})$	$\vec{\mu} \perp \vec{c}$, b*	2.4(3)	24.4
	30	$(0,0,0)$	$\vec{\mu} \perp \vec{c}$, B	5.8(1)	10.4
		$(\frac{1}{2},0,\frac{1}{2})$	$\vec{\mu} \perp \vec{c}$, b*	1.1(3)	62.9
0.6	2	$(0,0,0)$	$\vec{\mu} \perp \vec{c}$, C	8.1(1)	3.0
		$(\frac{1}{2},0,\frac{1}{2})$	$\vec{\mu} \perp \vec{c}$, c*	1.9(3)	29.2
	30	$(0,0,0)$	$\vec{\mu} \perp \vec{c}$, C	6.1(1)	8.5
		$(\frac{1}{2},0,\frac{1}{2})$	$\vec{\mu} \perp \vec{c}$, c*	0.9(3)	51.3
0.8	2	$(0,0,0)$	$\vec{\mu} \perp \vec{c}$, D	6.9(1)	5.9
		$(\frac{1}{2},0,\frac{1}{2})$	$\vec{\mu} \perp \vec{c}$, d	5.0(1)	6.8
	34	$(0,0,0)$	$\vec{\mu} \perp \vec{c}$, D	5.3(1)	6.3
		$(\frac{1}{2},0,\frac{1}{2})$	$\vec{\mu} \perp \vec{c}$, d*	1.0(2)	65.8
	54	$(0,0,0)$	$\vec{\mu} \perp \vec{c}$, D*	1.5(2)	52.5
0.9	2	$(0,0,0)$	$\vec{\mu} \perp \vec{c}$, D	6.1(2)	7.8
		$(\frac{1}{2},0,\frac{1}{2})$	$\vec{\mu} \perp \vec{c}$, d	6.0(1)	13.8
	32	$(0,0,0)$	$\vec{\mu} \perp \vec{c}$, D	4.7(1)	6.7
		$(\frac{1}{2},0,\frac{1}{2})$	$\vec{\mu} \perp \vec{c}$, d*	2.8(2)	23.0
	53	$(0,0,0)$	$\vec{\mu} \perp \vec{c}$, D*	2.4(2)	14.2
1.0	2	$(0,0,0)$	$\vec{\mu} \perp \vec{c}$, D	8.2(1)	9.4
		$(\frac{1}{2},0,\frac{1}{2})$	$\vec{\mu} \perp \vec{c}$, d*	2.7(2)	27.7
	34	$(0,0,0)$	$\vec{\mu} \perp \vec{c}$, D	6.7(1)	6.4
		$(\frac{1}{2},0,\frac{1}{2})$	$\vec{\mu} \perp \vec{c}$, d*	1.1(2)	44.3
	60	$(0,0,0)$	$\vec{\mu} \perp \vec{c}$, D*	2.5(2)	18.7

reach then the values between 8 and 9 μ_{B}. The moment arrangements which follow from the symmetry analysis[7] give worse agreement with the observed diffraction patterns. We note that the agreement factors for $\mathbf{k}_2$ components are rather high because of small intensities and frequent overlap with nuclear reflections, and hence also with magnetic peaks with the $(0,0,0)$ propagation.
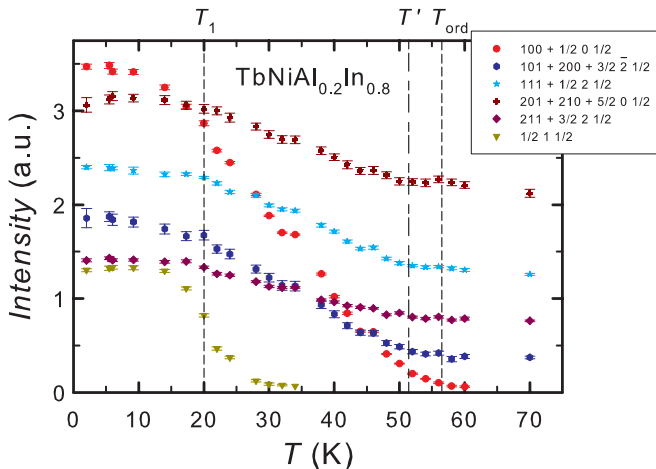
FIG. 7. (Color online) The temperature dependence of the intensity of the strongest reflections in TbNiAl$_{0.2}$In$_{0.8}$ compound. Dashed lines mark the temperatures of magnetic phase transitions as indicated by bulk measurements.[17]

The directions of total magnetic moments somewhat differ (approximately by about 20°) when comparing TbNiAl$_{0.2}$In$_{0.8}$ or TbNiAl$_{0.1}$In$_{0.9}$ and pure TbNiIn, although the magnetic structures corresponding to the $(0,0,0)$ and $(\frac{1}{2},0,\frac{1}{2})$ propagations are the same for all three concentrations. The value of the $(\frac{1}{2},0,\frac{1}{2})$ component is actually much lower for TbNiIn compared to the other two concentrations; the total magnetic structure is thus different. The vector sum for TbNiIn at 2 K is represented on Fig. 6(D + d).

Let us finally mention the magnetic phase transition that occurs slightly below T_{ord} in the In-rich compounds with $x \geqslant 0.8$ and is labeled as T' in Table II. This transition clearly shows up in the ac-susceptibility measurements[17] and is most probably related to some changes of the magnetic structure described by the $(0,0,0)$ propagation. As can be seen from Fig. 7, the intensity of (100) reflection starts to increase already at T_{ord}, whereas the intensities of (111), (201), and (210) seem to increase only below T'. The magnetic intensities around T' are, however, too small to allow exact determination of magnetic structure between T' and T_{ord}.
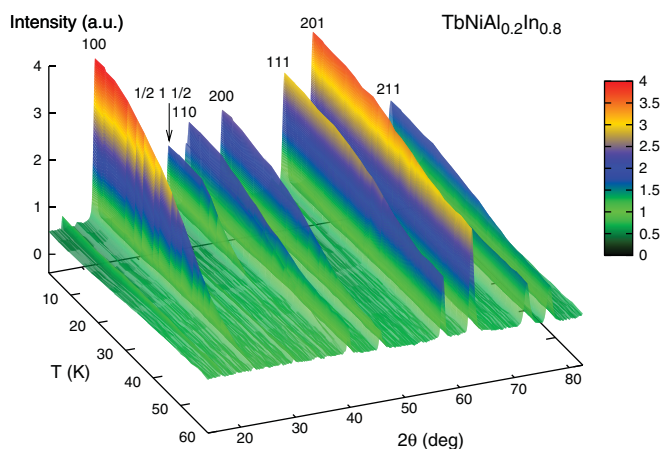

FIG. 8. (Color online) The temperature dependence of the diffraction pattern of TbNiAl$_{0.2}$In$_{0.8}$ compound.

IV. DISCUSSION

We observe the change of the antiferromagnetic arrangement of Tb moments in TbNiAl to predominantly ferromagnetic order with the substitution of 10% of Al by In. It is a further corroboration of the fact that the antiferromagnetic structure in TbNiAl is very unstable. The prevailing ferromagnetic coupling in the paramagnetic region is reflected by positive Curie-Weiss parameter[9] and the antiferromagnetic order can be easily disrupted by a magnetic field[7,13,14] or by various substitutions. The gradual transition to ferromagnetic structure was previously found also in Tb$_{1-x}$Y$_x$NiAl (Ref. 25) and TbNi$_{1-x}$Cu$_x$Al (Ref. 3) series. The substitution of Tb by a few percent of nonmagnetic Y disturbs the balance of magnetic moments, the substitution of Ni by Cu leads to a change of the electronic band structure as additional d-electrons are brought into the system. In our case, the Al-In substitution is isoelectronic, but the larger In atoms cause substantial changes of the structural parameters. The layer with the p-metal expands (lattice parameter a increases) and, consequently, the second layer can approach closer (lattice parameter c decreases) what results in a large decrease of the c/a ratio and volume increase with increasing the In content. The band structure can change as a consequence of such structural changes. Our result is well in agreement with the pressure-induced changes observed in Tb$_{1-x}$Y$_x$NiAl and TbNi$_{1-x}$Cu$_x$Al series[26]: The larger volume supports the ferromagnetic order.

The main aim of our study was the investigation of the change of magnetocrystalline anisotropy type. This change occurs between 40% and 50% of In substitution, that is, for slightly higher In concentrations than $\simeq$30% deduced originally from the low-temperature x-ray diffraction.[18] The small discrepancy can be explained by the fact that the x-ray experiment in magnetic field reflects the type and also to some extent the anisotropy energy. While the anisotropy type changes relatively suddenly, its energy develops more gradually. The strong uniaxial anisotropy of TbNiAl weakens with the increase of In content, that is, with the decrease of the c/a ratio, and the texture of the powder sample consequently disappears. The anisotropy in TbNiAl$_{0.6}$In$_{0.4}$ is still uniaxial, but induces only weak preferential orientation in 0.3 T used in the x-ray experiment.[18] On the other hand, the performed neutron diffraction experiment gives a direct observation of the moment direction in zero magnetic field and does not reflect the anisotropy energy.

The observed magnetic ordering results from the competition between exchange interactions, the geometrical frustration of the rare-earth magnetic moments and the influence of the crystal field. The latter affects the direction of magnetic moments and is usually responsible for the magnetocrystalline anisotropy in the rare earth compounds. The site symmetry on the Tb position in the ZrNiAl-type structure is orthorhombic $m2m$. The crystal field is then described by nine independent parameters, which is too large a number to be determined quantitatively, for example, by inelastic neutron diffraction.[10,27,28] The strongest anisotropy among this RTX family shows definitely the Tb-based compounds. We estimate the anisotropy energy from magnetization curves measured along different crystallographic directions of TbNiAl[7] and
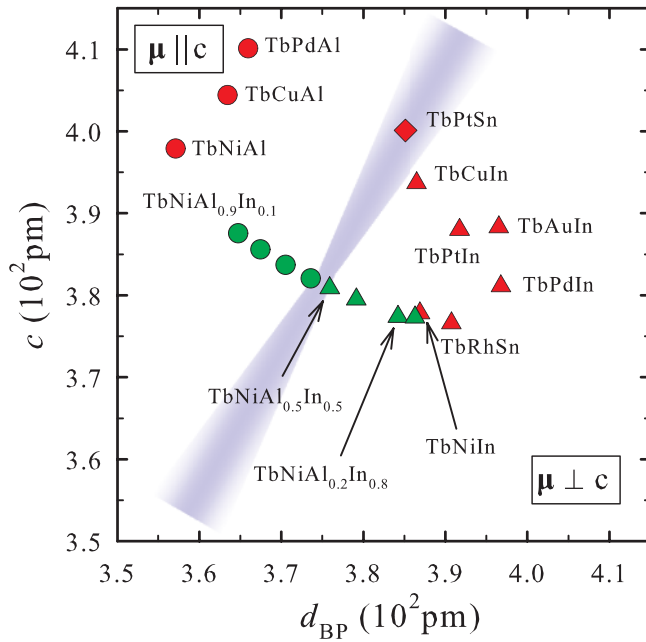
FIG. 9. (Color online) Magnetocrystalline anisotropy in Tb*TX* compounds related to the structural parameters. The compounds with Tb magnetic moments oriented along the c axis are denoted by circles, whereas compounds with Tb moments perpendicular to the c axis are denoted by triangles. The diamond corresponds to a magnetic structure with magnetic moments pointing out of any principal crystallographic direction. Following references for individual compounds were used to construct this figure: TbPdAl,[30,31] TbCuAl,[9] TbNiAl,[7] TbPtSn,[32] TbCuIn,[33] TbAuIn,[34] TbPdIn,[35] TbPtIn,[36,37] and TbRhSn.[38,39] The green symbols indicate data measured by neutron diffraction at 2 K in this work with the correct type of magnetocrystalline anisotropy. The gray area indicates assumed region of structural parameters where the magnetocrystalline anisotropy changes between uniaxial and planar type.

TbPtIn[29] to be about 70 K and 180 K in the $k_B T$ representation, respectively (see also comparison with other RPtIn compounds[29]). Taking into account all Tb*TX* compounds for which the magnetic structure was reported in the literature (see references below the Fig. 9), the clear tendency appears when drawing the anisotropy type, uniaxial or planar, in the plot of Tb-Tb distances, as shown in Fig. 9. The Tb moments are oriented along the c axis when the nearest Tb-Tb distances between the planes (parameter c) are large compared to those within the planes (d_{BP}), whereas Tb moments lie within the basal planes if c is small compared to d_{BP}. The relatively precise determination of the structural parameters where the magnetocrystalline anisotropy changes from the uniaxial to

the planar type in the TbNi(Al,In) series allows us to estimate the region where one can expect the change of the anisotropy type in Tb*TX* compounds in general. The TbPtSn compound showing more complex magnetic structure with Tb moments making an angle of 56° with the c axis[32] should also belong to this region.

The change of magnetic moment direction occurs here as a result of the change of crystal field parameters that generally depend on interatomic distances. The moment direction depends on the interatomic distances also in the uranium U*TX* compounds. The physical origin is, however, completely different. Here the mechanism of two-ion hybridization-induced anisotropy leads to the occupation of bonding $5f$ states pointing to the nearest U neighbor, that is, states with orbital moments perpendicular to nearest U-U links.[40] Unlike the rare-earth-based compounds, U*TX* compounds exhibit also a striking anisotropy of elastic properties,[41] which proves a different origin of the observed anisotropy.

V. CONCLUSIONS

Magnetic structures in the TbNiAl$_{1-x}$In$_x$ compounds were determined by powder neutron diffraction. The magnetic arrangement of Tb moments is characterized by two propagation vectors, $\mathbf{k}_1 = (0,0,0)$ and $\mathbf{k}_2 = (\frac{1}{2},0,\frac{1}{2})$, in the whole series. In the In-poor compounds ($x \leqslant 0.4$), the dominant ferromagnetic order with moments along the c axis develops first below the ordering temperature. The weaker basal-plane components with $\mathbf{k}_2$ appear then at lower temperatures. The antiferromagnetic order in TbNiAl is thus disrupted already for 10% In substitution. In the In-rich compounds ($x \geqslant 0.5$), both components lie within the basal plane and form complex noncollinear structure. The change of magnetocrystalline anisotropy from the uniaxial to planar type between 40% and 50% of In is a consequence of development of structural parameters in the studied series. The relation between anisotropy type and structural parameters seems to be general in the whole group of Tb*TX* compounds with the ZrNiAl type of structure. We draw a tentative picture that makes it possible to predict the moment direction on the basis of lattice parameters in this group of compounds.

*mi.klicpera@seznam.cz

[1] J. Prchal, P. Javorský, J. Rusz, F. de Boer, M. Diviš, H. Kitazawa, A. Dönni, S. Daniš, and V. Sechovský, Phys. Rev. B **77**, 134106 (2008).

[2] G. Ehlers and H. Maletta, Physica B: Condens. Matter **234–236**, 667 (1997).

[3] G. Ehlers, D. Ahlert, C. Ritter, W. Miekeley, and H. Maletta, Europhys. Lett. **37**, 269 (1997).

[4] J. Prchal, P. Javorský, M. Dopita, O. Isnard, and V. Sechovský, J. Alloys Compd. **408–412**, 155 (2006).

[5] J. Prchal, P. Javorský, J. P. Vejpravová, O. Isnard, B. Detlefs, S. Daniš, and V. Sechovský, Intermetallics **18**, 2109 (2010).

[6]S. Baran, A. Arulraj, D. Kaczorowski, B. Penc, and A. Szytuła, Intermetallics **18**, 42 (2010).

[7]P. Javorský, P. Burlet, V. Sechovský, A. V. Andreev, J. Brown, and P. Svoboda, J. Magn. Magn. Mater. **166**, 133 (1997).

[8]Ł. Gondek, A. Szytuła, S. Baran, and J. Hernandez-Velasco, J. Magn. Magn. Mater. **272–276**, e443 (2004).

[9]G. Ehlers and H. Maletta, Z. Phys. B **99**, 145 (1996).

[10]P. Javorský, J. Prchal, and D. Adroja, Solid State Commun. **146**, 21 (2008).

[11]N. K. Singh, K. G. Suresh, R. Nirmala, A. K. Nigam, and S. K. Malik, J. Magn. Magn. Mater. **302**, 302 (2006).

[12]G. Ehlers, H. Casalta, R. E. Lechner, and H. Maletta, Phys. Rev. B **63**, 224407 (2001).

[13]G. Ehlers, C. Ritter, J. R. Stewart, A. D. Hillier, and H. Maletta, Phys. Rev. B **75**, 024420 (2007).

[14]J. Kaštil, P. Javorský, and J. Pospíšil, J. Alloys Compd. **509**, 5931 (2011).

[15]Y. B. Tyvanchuk, Y. M. Kalyczak, Ł. Gondek, M. Rams, A. Szytuła, and Z. Tomkowicz, J. Magn. Magn. Mater. **277**, 368 (2004).

[16]H. Zhang, Z. Y. Xu, X. Q. Zheng, J. Shen, F. X. Hu, J. R. Sun, and B. G. Shen, J. Appl. Phys. **109**, 123926 (2011).

[17]M. Klicpera, P. Javorský, and E. Šantavá, Acta Physica Polonica A **118**, 881 (2010).

[18]M. Klicpera, P. Javorský, and S. Daniš, J. Phys.: Conf. Ser. **303**, 012031 (2011).

[19]J. Rodriguez-Carvajal, Physica B **192**, 55 (1993).

[20]V. F. Sears, Neutron News **3**, 26 (1992).

[21]A. March, Zeitschrift für Kristallographie **81**, 285 (1932).

[22]A. S. Wills, Physica B **276–278**, 680 (2000).

[23]P. Javorský, H. Sugawara, D. Rafaja, F. Bourdarot, and H. Sato, J. Alloys Compd. **323**, 472 (2001).

[24]J. Prchal, P. Javorský, K. Prokeš, B. Ouladdiaf, and A. V. Andreev, Physica B **385–386**, 346 (2006).

[25]G. Ehlers, C. Ritter, A. Krutjakow, W. Miekeley, N. Stüsser, T. Zeiske, and H. Maletta, Phys. Rev. B **59**, 8821 (1999).

[26]G. Ehlers, C. Ritter, K. Knorr, R. Schneider, D. Hohlwein, M. Meissner, and H. Maletta, Physica B **276–278**, 650 (2000).

[27]P. Javorský, M. Diviš, H. Sugawara, H. Sato, and H. Mutka, Phys. Rev. B **65**, 014404 (2001).

[28]Ł. Gondek, J. Czub, A. Szytuła, Z. Izaola, and E. Kemner, Solid State Commun. **149**, 1596 (2009).

[29]E. Morosan, S. L. Bud'ko, and P. C. Canfield, Phys. Rev. B **72**, 014425 (2005).

[30]P. Javorský, J. Prokleška, O. Isnard, and J. Prchal, J. Phys. Condens. Matter **20**, 104223 (2008).

[31]A. Dönni, H. Kitazawa, L. Keller, P. Fischer, P. Javorský, F. Fauth, and M. Zolliker, J. Alloys Compd. **477**, 16 (2009).

[32]A. Szytuła, M. Kolenda, J. Leciejewicz, and N. Stüsser, J. Magn. Magn. Mater. **164**, 377 (1996).

[33]A. Szytuła, A. Arulraj, S. Baran, T. Jaworska-Gołab, B. Penc, N. Stüsser, Y. Tyvanchuk, and A. Zarzycki, Acta Physica Polonica A **113**, 1185 (2008).

[34]A. Szytuła, W. Bażela, Ł. Gondek, T. Jaworska-Gołab, B. Penc, N. Stüsser, and A. Zygmunt, J. Alloys Compd. **336**, 11 (2002).

[35]P. Javorský, J. Fikáček, J. Prokleška, S. Nishigori, and G. J. M. Intyre, Acta Physica Polonica A **118**, 879 (2010).

[36]O. Garlea, E. Morosan, S. Bud'ko, J. Zarestky, P. Canfield, and C. Stassis, J. Appl. Phys. **95**, 6921 (2004).

[37]E. Morosan, S. L. Bud'ko, and P. C. Canfield, Phys. Rev. B **71**, 014445 (2005).

[38]A. Szytuła, B. Penc, and E. Ressouche, J. Alloys Compd. **244**, 94 (1996).

[39]S. Baran, M. Bałanda, P. Fischer, W. Sikora, and A. Szytuła, J. Magn. Magn. Mater. **261**, 369 (2003).

[40]L. Havela, V. Sechovský, F. de Boer, E. Brück, and H. Nakotte, Physica B **177**, 159 (1992).

[41]L. Havela, M. Diviš, V. Sechovský, A. Andreev, F. Honda, G. Oomi, Y. Méresse, and S. Heatman, J. Alloys Compd. **322**, 7 (2001).